Журнал нано- та електронної фізики
Том **7** № 4, 04025(4cc) (2015)

Journal of Nano- and Electronic Physics
Vol. **7** No 4, 04025(4pp) (2015)

An Analysis of the Deposition Process and the Structure of Ferroelectric Langmuir Films of Barium Titanate

A.P. Kuzmenko[1,*], I.V. Chuhaeva[1], P.V. Abakumov[1], M.B. Dobromyslov[2], N.A. Emelyanov[3]

[1] *South-West State University, 94, 50 let Octyabrya St., 305040 Kursk, Russia*
[2] *Pacific National University, 136, Tihookeanskaya St., 680035 Khabarovsk, Russia*
[3] *Kursk State University, 33, Radisheva St., 305000 Kursk, Russia*

(Received 23 September 2015; published online 10 December 2015)

The paper analyzes the process of formation and subsequent deposition of monolayers stabilized in sodium oleate nanoparticles of barium titanate. X-ray diffractometer studies conducted particle size distribution of the ferroelectric particles deposited. Probe technique was used to study the effect of matter and the wettability of the underlayer on the structure and quality of deposited coatings. The possibility of recording ferroelectric domains produced thin Langmuir films of barium titanate.

Keywords:: Langmuir-Blodgett films, Scanning microscopy, Scanning probe microscopy, Surface potential, π-A isotherms, Ferroelectric.

PACS numbers: 68.18. – g, 68.47.Pe, 68.37.Ps, 85.50. – n

Synthesis of monolayered materials of organic, non-organic, and mixed nature is of great interest, which is due to the necessity of obtaining unique set of features needed in various fields of science and engineering [1]. A lot of methods for producing such materials exist (direct synthesis, crystallization, self-organization, etc.) but the Langmuir-Blodgett method (LB) is of most interest at present. The method makes it possible to produce thin films of a set thickness without special conditions: vacuum, high temperatures and pressures, degassing. Fat acids and their salts are the typical materials for Langmuir films. These are amphiphilic to produce stabilized monolayers. For a number of challenges, it is necessary to obtain thin films from materials not diphilic but having needed features. One of those materials is barium titanate, $BaTiO_3$, (BTO). BTO is ferroelectric with photorefractive and piezoelectric effects, featuring super high permittivity, high Curie temperature (120 °C), thermo- and mechanical resistance, and also electrooptic and dielectric properties [2]. Unique properties of BTO are used in capacitors, optoelectronic devices, piezoelectric transducers, and MEMS devices [3].

The present paper has determined optimum deposition parameters of stabilized BTO particles with LB method. Also, temperature dependencies of π-A isotherms, the hysteresis of compression-extension processes and changes in the surface potential are analyzed. The influence of substrates on the quality of deposited BTO films and polarizability of a thin barium titanate film according to electrostatic force microscopy are studied.

To produce Langmuir monolayers, BTO nanoparticles of an almost spherical shape obtained by peroxide synthesis in tetragonal and cube phase were used [4]. Stabilization of nanoparticles was achieved by saturation of their surfaces with hydroxyl groups OH with boiling in 30 % hydrogen peroxide solution for three hours. Hydroxylated nanoparticles obtained were also modified with sodium oleate $C_{17}H_{33}COONa$ molecules by vigorous agitation in 0.5 % water solution at 85 °C for four hours as in [5, 6]. Homogeneity of colloidal BTO solutions was enhanced at centrifuge MiniSpin plus, Eppendorf.

Investigations were conducted with plant KSV NIMA 2002 [7] that featured built-in thermostat JULABO F12-ED ((– 20÷ +100) ± 0.03 °C) and device (SPOT) for surface potential measurement (300 Hz, 1 mV). The formation was visualized with Brewster microscope MicroBAM (resolution 12 μm). π-A isotherms (error 5 μN/m) and surface potential were obtained with discretization period of slightly more than 1 s, and the total number of points was several thousands. Morphology of BTO monolayers was examined with atomic-force microscope (AFM) AIST-NT in a semi contact mode (cantilever with standard silicon probe). Particle size distribution DV(r) was plotted based on data of small-angle X-ray scattering (SAXS) that were obtained at plant SAXSess mc^2 (Anton Paar, Austria) in a linear collimation mode (Cu Kα with a wavelength of 0.154 nm within range from 0.03 to 28 nm^{-1} with a resolution of 0.03 nm^{-1}). Ferroectric properties of monolayers were studied at SPM NTegra Aura (NT-MDT) with platinum coating conductive probe.

Particle size distribution DV(r) according to SAXS is given in Fig. 1. As is seen, averaged radii of synthesized particles were 5, 12, and 27 nm.

For optimization of deposition parameters of BTO πA isotherms were constructed at various BTO volumes, barrier velocities, and temperatures. Thus, the rational parameters of deposition are the following: volume – 3 μl, the barrier velocity – 5 mm/min, pressure of transfer – 25 mN/m, temperature – 295 K.

Analysis of images in microscope MicroBAM [8] reveals that (Fig.2) monolayer begins its formation even at $\pi = 0.16$ mN/m. In doing so, drop-like structures start to form the size of up to 120 μm that are divided by small water areas. Beginning with $\pi = 9$ μm, they are

* apk3527@mail.ru

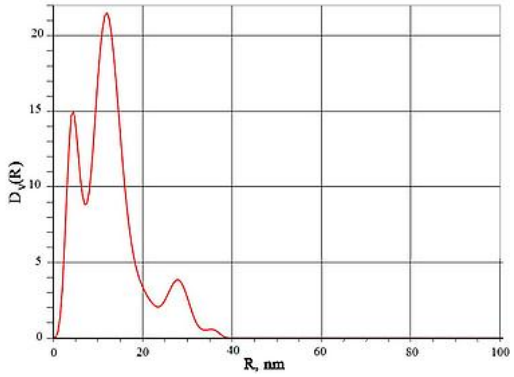

Fig. 1 – Granulometric analysis of BTO nanoparticles

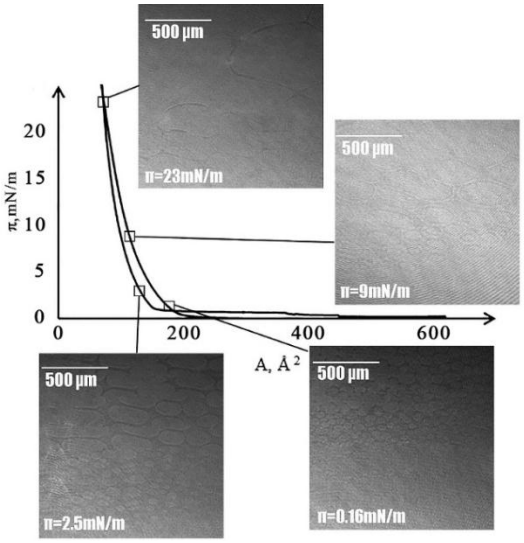

Fig. 2 – Data of angle Brewster microscopy at compression-extension of BTO monolayer

joined to produce ellipsoid-like structures with axes of the order of 200 and 400 μm. At a pressure of 25 mN/m, a compact monolayer is formed. The further pressure increase did not produce collapse, which is probably due to the transfer of particles from the water surface into internal layers of the subphase. This is supported by the film destruction at its extension starting with $\pi = 2.5$ mN/m.

As is seen from images of MicroBAM, at temperatures of 283 and 310 K the formation of nonzero thickness domains occurs only to the surface pressure of $\pi = 0.3$ mN/m (Fig. 3). With further increase in pressure at such temperatures monolayers do not form. At the start of film formation at a temperature of 295 K, the domain area is not large and the domains are located far away from each other. At this temperature with pressure increasing domains are joined to produce a uniform monolayer. According to the classification [9], the nature of isotherms corresponds to the "gas-solid" phase transition. Brewster images of monolayers (Fig. 3) at $T = 283$, 310, and 295 K are noticeably different, which is indicative of an essential temperature effect on phase transitions at BTO monolayer formation.

Measurement of π-A isotherms and the surface potential given in Fig. 4 were conducted during two contraction-extension cycles of a monolayer under study.

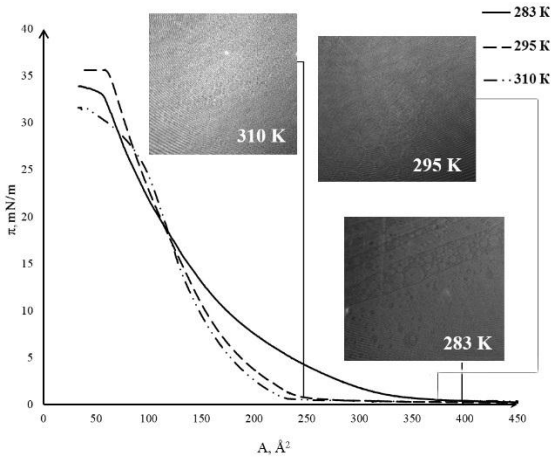

Fig. 3 – Microscopy under Brewster angle of BTO monolayers at various temperatures ($\pi = 0.3$ mN/m)

With every cycle, an increase in area per molecule was noted (at contraction from 290 Å² to 380 Å², at an extension from 240 Å² to 300 Å² at a pressure of 25 mN/m). This may be explained by the domain formation, which impedes the successive film decay into individual particles at its extension. The inferences obtained from analysis of united π-A dependencies and surface potential that provide a qualitative picture about phase transitions and the processes of both formation and destruction of the monolayer are in accord with inferences [10].

At contraction, a sharp increase in surface potential is observed, which corresponds to the onset of film formation and is corroborated by Brewster microscopy. Relative to the point of surface potential increase, the area per molecule before the film formation in the first cycle is 454 Å², whereas at the second cycle – 474 Å² (Fig. 4).

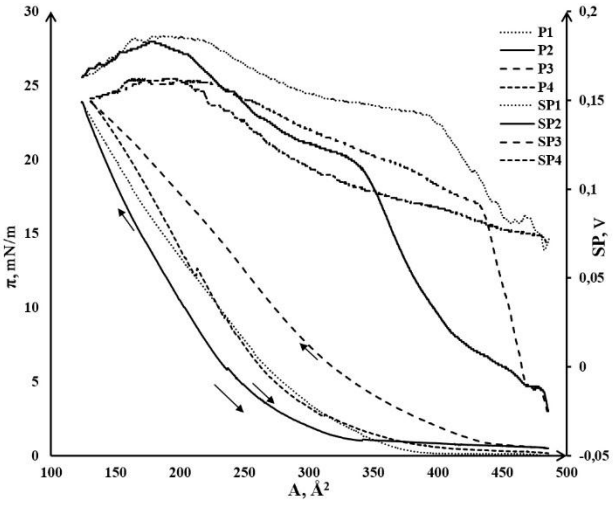

Fig. 4 – Hysteresis of contraction-extension (1) and surface potential (2) for BTO

The surface potential for the second cycle is reduced by 0.08 V. At greater number of cycles, the similar dependence occurs, that is surface potential of the monolayer is reciprocally proportional to the area per molecule in accord to the inferences [11]:

$$\Delta U = \mu/(\varepsilon_0 \varepsilon_1 A) \quad (1)$$

where μ is a vertical component of the dipole momentum, ε_0 is the dielectric constant, ε_1 is permittivity of the monolayer, A is the area per molecule. Of note is the fact that according to (1), from measured ΔU and A, with consideration for values of ε_1 a vertical component of the dipole momentum μ may be determined.

With consideration for [12], the role of both quality of substrate surface and their structure in the LB formation of BTO monolayers was considered. To this end, the substrates of amorphous (glass), single crystal (silicon KDB (100)) and poly crystal at a glass from magnetron films Pt and Ni with Cr were prepared. Deposition of monolayered LB films from stabilized BTO was conducted by the vertical lift with consideration for the noted parameters of deposition by transfer of distilled water from the surface to the substrates. The total number of philic substrates was 7, for hydrophobic substrates – 8. The values of BTO transfer coefficients to the substrates under study, which were determined by the difference $S - S'$ – areas before and after transfer of BTO to the substrate with respect to the substrate area – S_π:

$$k = (S - S') / S_\pi$$

turned out to be different. Their values are given in Table 1. The closest to unity transfer coefficient was for Pt substrate, which may be indicative of uniformity of the BTO monolayer formed.

Table 1 – Transfer coefficients of LB films of BTO to various substrates

Substrate	Glass	Si	Pt	Ni
Transfer coefficient	0.6-1.19	0.4-1.1	0.9-1.2	0.1-0.3

AFM-images of surfaces and one of profilograms for the substrates under study and formed on them BTO monolayers are shown in Fig. 5. As is well known, magnetron coatings are characterized in the deposition process by the formation of cluster structures, which is supported by Fig. 5, I and II). The comparison of images before (Fig. 5, I and II) and after deposition of BTO (Fig. 5, I′ and II′) shows that for Pt the initial cluster structure was fully covered with nearly-the-same size nanoparticles as regular rows. At the same time, for Ni, clusters are evidently observed. It should be noted that the AFM-images of the original surfaces of glass and silicon are without clusters. After BTO deposition, nanoparticles do not become more ordered, which is seen from the comparison of images before (Fig. 5, III and IV) and after BTO deposition (Fig. 5, III′ и IV′).

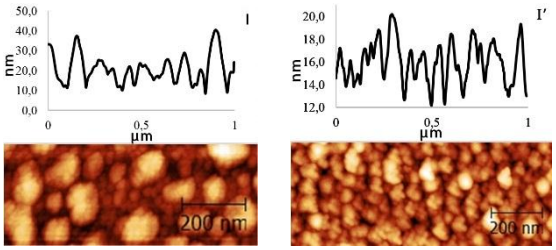

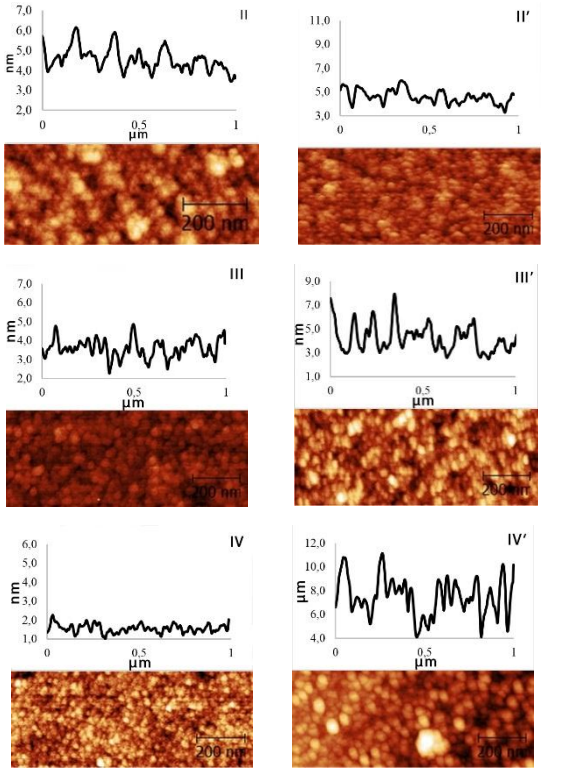

Fig. 5 – AFM-images of topology of substrate surfaces from Pt – I, Ni – II, glass – III and silicon – IV and BTO monolayers (vertical deposition) onto magnetron films Pt – I′ and Ni – II′, and substrates from glass – III′ and silicon – IV′

The results of the granulometric analysis of BTO monolayer surfaces are given in Table 2. Average size of BTO particles coincide at deposition onto Pt and Si substrates (Fig.5, I′ and IV′), which correlates with the transfer coefficient value (Table 1) and is supported by the surface profiles where changes in height turned out to be equal and were 7 nm. For a film at the substrate with magnetron film nickel with transfer coefficient significantly smaller than unity (Table 1) AFM-image (Fig. 5, II′) demonstrates that BTO particles virtually coincide in size with size of the film structures at the substrate itself.

Table 2 – Topological size of substrate surface before and after BTO deposition

Substrate type	Average particle size, nm	
	Substrate	Film
Platinum / glass	10	7
Nickel / Glass	5	6
Glass	4	4
Silicon	2	7

Reasonably high value of $k = 0.6–1.19$ might be expected to cause the film formation onto the glass. However, average size characterized both the glass surface itself and possible deposition of BTO particles onto it turns out to be equal.

To determine the fact of BTO deposition onto glass as well as other substrates, with an optical microscope by drop projection wetting angles θ were measured that are given in Table 3. It proved to be that Pt and Si

substrates had the least values of θ whereas its value for Ni and glass increased several times although did not reach $\pi/2$. This fact may be indicative either of pure quality of a formed film or, in general, its absence at all. This conclusion is in accord with data from Table 2 where just on these substrates the average characteristic size after BTO deposition for glass did not change, and for Ni differed slightly – 1 nm (accuracy of measurement was 20 pm).

Table 3 – The wetting angle of colloidal solution of BTO onto substrates under study

Substrate for BTO deposition	Glass	Ni	Si	Pt
Wetting angle, θ (deg.)	67°	55°	35°	10°

The results on BTO deposition at various substrates under equal conditions, as is shown in Table 1-3 and Fig. 5, are indicative of the fact that the LB films of BTO are of higher quality at Platinum substrate.

Thus, to study the ferroelectric properties of the films was selected substrate with a platinum sublayer.

Using microscopy piezoelectric response the film surface with an area of 5×5 μm^2 was polarized with a constant voltage of record of ± 10 V according to the scheme "cantilever-film-substrate". By scanning in the mode of a kelvin probe microscopy on the bigger area of a film – 10×10 μm^2, the high level of polarization was established (Fig. 6).

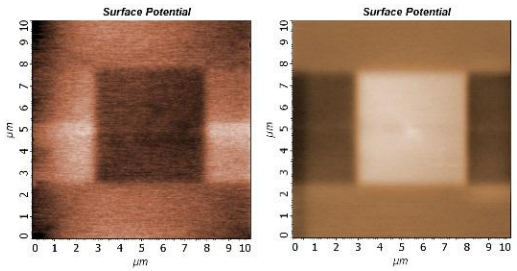

Fig. 6 – Spatial distribution of surface potential for the polarized BTO at the record with voltage: left – 10 V and right – + 10 V

The observed "dark" and "light" areas correspond to ferroelectric domains with the polarization vector directed from a probe and to it, respectively. Spatial localization at the record was comparable to the radius of the cantilever probe with the conducting covering ~ 100 nanometers.

Thus, optimum parameters of the stabilized BTO sedimentation were set by the LB method; the influence of a substrate on the structure of the created BTO films is studied. The polarization of the coverings obtained which is characterized by high level of both contrast and spatial localization is found.

REFERENCES

1. N.G. Suhodolov, N.S. Ivanov, E.P. Podolskaya, *Nauchnoe priborostroenie* **23**, 1 (2013) [In Russian].
2. Burcu Ertug, *Am. J. Eng. Res.* **2**, 1 (2013).
3. C.C. Li, S.J. Chang, J.T. Lee, *Colloid. Surf. A* **361**, 143 (2010).
4. A.P. Kuzmenko, et al., *J. Nano- Electron. Phys.* **5** No 4, 04019 (2013).
5. C.C. Li, S.J. Chang, J.T. Lee, W.S. Liao, *Colloid. Surf. A* **361**, 143 (2010).
6. S. Chang, W. Liao, C. Ciou, J. Lee, C. Li, *J. Colloid. Interf. Sci.* **329**, 300 (2009).
7. A.P. Kuzmenko, I.V. Chuhaeva, M.B. Dobromyslov, *J. Nano- Electron. Phys.* **5** No 4, 04035 (2013).
8. E.P. Mironov, et al., *VMC Physics Astronomy* **6** (2013) [In Russian].
9. R.H. Tredgold, *The physics of Langmuir-Blodgett films* 50, (1987).
10. A.M. Yashenok, et al., *Semiconductors* **41**, 684 (2007).
11. L.M. Blinov, *Phys.-Usp.* **31**, 623 (1988).
12. V.V. Rozanov, A.A. Evstrapov, *Nauchnoe Priborostroenie* **17**, 4 (2007) [In Russian].
13. L.V. Blinov V.M. Fridkin, S.P. Palto, *Phys.-Usp.* **43**, 243 (2000).
14. V.M. Fridkin, *Phys.-Usp.* **49**, 193 (2006).
15. R.V. Gaynutdinov, et al., *JEPT Lett.* **98** No 6, 339 (2013).
16. P. George, et al., *Nanoscale Res. Lett.* **62**, 8 (2013).